HULL FORM OPTIMISATION FOR IMPROVED HYDRODYNAMIC PERFORMANCE

Mac-Pepple Blessing James[1], Azubuike John Chuku[1], Charles Ugochukwu Orji[1]

[1]*Department of Marine Engineering, Rivers State University, Port Harcourt, Nigeria.*

Abstract - *Analytical method has been used to perform the optimization of bourbon Helene using the response amplitude operator (RAOs) from Structural Analysis Computer system (SACs). MATLAB was used in simulating the optimization process. Initial resistance values extracted from SACs motion analyses were used as the input values in comparing the resistance and power as against the vessel forward speed at 180 Degree and 135 Degree respectively. Main dimensions of the ship were used to generate various hull models and Autodesk inventor deployed to model the various vessel hull forms. The optimization was to improve on the vessel hydrodynamic performance of MV Helene in calm water in order to achieve good sea-keeping condition, reduced resistance, enhanced maneuverability and consequently reduced fuel consumption at 0,5,10,15,20,23 and 25 knots forward speed on regular sea wave condition of 4m. The hull form optimization was meant after a boubous bow was designed on the forward part of the ship hull using SACs modeler by adjusting and dragging the hull NURB surfaces to achieve the defined hull form which is used for the various analysis. After comparing the initial hull form predicted RAOs response and resistance values to the optimized hull form values, results shows that there was a significant reduction in the optimized RAOs response and resistance values which were subsequently used to estimate and compare the optimized and initial effective power to speed of the vessel.*

***Key Words*: Hull form, optimization, performance, vessel.**

1.INTRODUCTION

The work investigated the extent to which hull design can influence the sea keeping response. The optimization procedures were based on the assumption that the optimum hull is found when the vertical plane motions and absolute vertical acceleration in regular head waves due to combined pitch and heave motions are minimized. More than 70% of the earth is covered by water, ever since humans uncovered the principles of buoyancy, moving from place to place using flotation attracted serious attention and exploitation. More than 10,000 years ago, humans found ways to refine the shapes of floating logs which resulted in the construction of canoes. Later, rafts were created by joining a number of logs together which allowed for a greater payload, the design of vessels using the assembly of wooden planks to construct a hull form was perfected by the ancient Egyptians around 3000 BC, [12]. The Greeks, Swahilis and Chinese made use of their uniquely designed ships to discover new lands, engage in trade and establish dominance. Ship design and building activities have spanned time with unique designs evolving in different parts of the world. The Romans, Vikings, English, Spanish and Japanese built different styles of fleets, their various designs evolved slowly and characterized as being more an art, than a science. Today, the ship design process has evolved to a well-structured science-based discipline. Evans introduced a formal model of the ship design process i.e., the ship design spiral in 1959 which captured the basic principles in designing a ship using an iterative process. It follows those ships are designed based on providing functional capability (e.g., transport, military, recreation, etc.) while satisfying the set of constraints arising from statutory requirements, physical laws etc. Several enhancements have been introduced to the spiral, including the inclusion of time and economic dimensions. However, the ship design spiral approach results in a feasible design and not necessarily an optimum. A shift from sequential and iterative (i.e., design spiral) to simultaneous considerations of the performance indicators was proposed by Lyon in 1976 through the incorporation of optimization techniques. Such a shift in design practice provided an opportunity for ship designers to produce near optimum, rather than simply feasible designs. In recent years bulk careers, tankers and RoRo ships have received quite a lot of attention from the maritime community whilst still more needs to be done in those areas that only causes for concern. Many if not most of the ships lost will have been built, maintained and manned in accordance with the latest rules and regulations adopted by IMO in 2000. A ship's hull form helps determine most of its main attributes, its stability characteristics, its resistance and therefore the power needed for a given speed, its sea worthiness, its maneuverability and its load carrying capacity, [11]. It is therefore important, that the hull shape should be defined with some precious and unambiguously for good hydrodynamic performance to achieve the basic descriptors which must be defined. The ship's hull is three dimensional and except in a very few cases is symmetrical about a fore and aft plane, the hull shape is defined by its intersection with three sets of mutually orthogonal plane. The horizontal planes are known as water plane and the lines of intersection are known as waterlines, the planes parallel to the middle line plane itself defining the profile, while the intersection of the athwart ships plane defines the transverse section, [1].

1.2 Objective of this Research Work

- To estimate the required power due to pressure resistance on the ship hull
- To achieve optimum values of hydrodynamic parameters, design service speed, Resistance and required hull form modification.
- To provide knowledge at a basic level for those whose responsibilities include hull form design.
- To establish the required hull form to withstand the loads imposed upon it from the weight of cargo, hydrodynamic pressures and impact forces induced by waves.

1.3 Aim of this Research

The improvement for standards of performance evaluation is analyzed using the selected optimal design case, the performance of the optimized hull form is better than that of the original parent hull form in terms of stability and resistance. Discovering of certain tool that will allow the designer to predict the given hull form to be used for global optimization purpose and efficient computational time to enable the designer to quickly update the design due to changing requirements once the optimal hull design is established, then designer can move to higher fidelity code to define the hull.

2. METHODOLOGY

2.1 Methods

2.1.1 Numerical Analytical Development Procedure

The ship is considered to be a rigid body, floating on the surface of an ideal fluid, which is homogeneous, incompressible, free of surface tension, irrotational and without viscosity. It is assumed that the problem of the motions of this floating body in waves is linear or can be linearized. Consequently, only the external loads on the underwater part of the ship are considered here and the effect of the above water part will be fully neglected, [2]. An overview of sea keeping theories for ships were presented and it was concluded that - nevertheless some limitations strip theories are the most successful and practical tools for the calculation of the wave induced motions of the ship, at least in an early design stage of a ship. The strip theory solves the three-dimensional problem of the hydromechanical and exciting wave forces and moments on the ship by integrating the two-dimensional potential solutions over the ship's length. Interactions between the cross sections are ignored for the zero-speed case. So, each cross section of the ship is considered to be part of an infinitely long cylinder, [3].

The still water level is the average water level or the level of the water if no waves were present. The x-axis is positive in the direction of wave propagation. The water depth, *h*, (a positive value) is measured between the seabed (z = -*h*) and the still water level (z = 0). The highest point of the wave is called its crest and the lowest point on its surface is the trough. If the wave is described by a harmonic wave, then its amplitude ζ_a is the distance from the still water level to the crest, or the trough for that matter. The subscript *a* denotes the amplitude, here.

The horizontal distance (measured in the direction of wave propagation) between any two successive wave crests is the wavelength, λ. The distance along the time axis is the wave period, *T*. The ratio of wave height to wavelength is often referred to as the dimensionless wave steepness:

$$2.\zeta_a / \lambda. \tag{2.0}$$

Since the distance between any two corresponding points on successive harmonic waves is the same, wave lengths and periods are usually actually measured between two consecutives upward (or downward) crossings of the still water level. Such points are also called zero crossings, and are easier to detect in a wave record.

Since sine or cosine waves are expressed in terms of angular arguments, the wavelength and wave period are converted to angles using:

$$k.\lambda = 2.\pi \quad \text{or} \quad k = \frac{2.\pi}{\lambda}$$
$$\omega.T = 2.\pi \quad \quad \omega = \frac{2.\pi}{T} \tag{2.1}$$

In which *k* is the wave number (rad/m) and is the circular wave frequency (rad/s).

Obviously, the wave form moves one wave length during one period, so that it speed or phase velocity, c, is given by:

$$c = \frac{\lambda}{T} = \frac{\omega}{k} \tag{2.2}$$

Another right-handed co-ordinate system $o(x, y, z)$ is moving forward with a constant ship speed *V*. The directions of the axes are: x in the direction of the forward ship speed *V*, *y* in the lateral port side direction and z vertically upwards. The ship is supposed to carry out oscillations around this moving $o(x, y, z)$ co-ordinate system. The origin O lies vertically above or under the time-averaged position of the centre of gravity G. The $(x, y,)$ -plane lies in the still water surface.

A third right-handed co-ordinate system $G(x_b, y_b, z_b)$ is connected to the ship with its origin at G, the ship's centre of gravity. The directions of the axes are: x_b in the longitudinal forward direction, y_b in the lateral port side direction and z_b upwards. In still water, the (x_b, y_b)-plane is parallel to the still water surface.

If the wave moves in the positive x_0-direction (defined in a direction with an angle μ relative to the ship's speed vector, V), the wave profile – the form of the water surface – can now be expressed as a function of both x_0 and t as follows:

$$\zeta = \zeta_a \cos(k.x_0 - \omega.t - k.x_0) \quad (2.3)$$

The right-handed co-ordinate system $O(x, y\, z)$ is moving with the ship's speed V, which yields:

$$x_0 = V.t.\cos\mu + x.\cos\mu + y.\sin\mu$$

From the relation between the frequency of encounter ω_e and the wave frequency ω: $\omega_e = \omega - k.V.\cos\mu$ follows:

$$\xi = \xi_a.\cos(\omega_e.t - k.\cos\mu - k.y.\sin\mu \quad (2.4)$$

The resulting six ship motion in the $O(x, y, x)$ system is defined by three translations of the ship's centre of gravity in the direction of the $x-, y-$ and z-axes and three rotations about them:

Surge: $x = x_a.\cos(\omega_e.t + \varepsilon_{x\zeta})$ (2.5)

Sway: $y = y_a.\cos(\omega_e.t + \varepsilon_{y\zeta})$ (2.6)

Heave: $z = z_a.\cos(\omega_e.t + \varepsilon_{z\zeta})$ (2.7)

Roll: $\phi = \phi_a.\cos(\omega_e.t + \varepsilon_{\phi\zeta})$ (2.8)

Pitch: $\theta = \theta_a.\cos(\omega_e.t + \varepsilon_{\theta\zeta})$ (2.9)

Yaw: $\psi = \psi_a.\cos(\omega_e.t + \varepsilon_{\psi\zeta})$ (2.10)

2.1.2 Jonswap Spectrum

This criterion is used in places where the wave formation region is a constraining factor for wave generation, it is a variation of the Brettschneider spectrum. Sea keeping analyses is the ability of how well a vessel is to condition when underway. It also refers to the analyzing of the behavior of a vessel in regular and irregular waves, represented through the RAOs (Response Amplitude Operator). RAO is a linear operator that represents the input (wave) – output (movement) transfer, it being of key relevance to determine vessel design parameters, [5]. The RAO describes how the response of the vessel changes with frequency variations. The various graphs in chapter 4 shows a classic example of a RAO response representing the Heave, Pitch and Roll amplitudes from the PSV Case study. We can see how RAO approaches one for low frequencies and it is when the vessel shifts up and down with the wave, acting as a cork for high frequencies, the response approaches zero while the effect of many short waves is cancelled along the vessel's length. From analysis of the measured spectra, a spectral formulation of wind generated seas with a fetch limitation was found. The following definition of a mean JONSWAP wave spectrum is advised by the 15th ITTC in 1978 for fetch limited situations:

$$S_\zeta(\omega) = \frac{172.8.H_{1/3}{}^2.\omega^{-5}}{}.\exp\{\frac{-691.2}{T_1^3}.\omega^4\}.A.r^5 \quad (2.11)$$

With

$$A = 0.658^5$$

$$B = \exp\left\{\left(\frac{\frac{\omega}{\omega_p} - 1.0}{\sigma.\sqrt{2}}\right)\right\}$$

$r = 3.3$ peakedness factor

$$\omega_p = \frac{2.\pi}{T_p} \quad (\text{circular frequency at spectral peak})$$

$\sigma = a$ step function of ω: if $\omega < \omega_p$ then: $\sigma = 0.0.7$

if $\omega > \omega_p$ then: $\sigma = 0.09$

The JONSWAP expression is equal to the Brettschneider definition multiplied by the frequency function $A.r^B$.

Sometimes, a third free parameter is introduced in the JONSWAP wave spectrum by varying the peakedness factor r.

The n^{th} order spectral moments of the wave spectrum, defined as a function of the circular wave frequency w, are:

$$m_{n\zeta} = \int_0^\alpha S_\zeta(\omega).\omega^n.d\omega \quad (2.12)$$

The breadth of a wave spectrum is defined by:

$$\varepsilon = \sqrt{1 - \frac{m_{2\zeta}{}^2}{m_{0\zeta}.m_{4\zeta}}}$$

The significant wave height is defined by:

$$H_{1/3} = 4.\sqrt{m_{0\zeta}} \quad (2.13)$$

The several definitions of the average wave period are:

T_p peak or modal wave period, corresponding to peak of spectral curve

$T_1 = 2.\pi.\frac{m_{0\zeta}}{m_{1\zeta}}$ average wave period, corresponding to centroid of spectral curve

$T_2 = 2.\pi.\sqrt{\frac{m_{0\zeta}}{m_{1\zeta}}}$ average zero-crossing wave period, corresponding to radius of inertia of spectral curve

$$\left.\begin{array}{lllll} T_1 & = & 1.073.T_2 & = & 0.834.T_p \\ 0.932.T_1 & = & T_2 & = & 0.777.T_p \\ 1.199.T_1 & = & 1.287.T_2 & = & .T_p \end{array}\right\} \text{ for}$$

JONSWAP wave spectra

Truncation of wave spectra during numerical calculations can cause differences between input and calculated wave periods. Generally, the wave heights will not differ much.

The energy spectrum of the responses $r(i)$ of a sailing ship in the regular waves follows from the transfer function of the response and the wave energy spectrum by:

$$S_r(\omega)=\left(\frac{r_a}{\zeta_a}\right)^2.S_\zeta(\omega) \quad or \quad S_r(\omega_e)=\left(\frac{r_a}{\zeta_a}\right)^2.S_\zeta(\omega) \tag{2.14}$$

The moments of the response spectrum are given by:

$$m_{nr} = \int_0^\alpha S_r(\omega).\omega_e^n \tag{2.15}$$

$$with: n = 0,1,2\ldots$$

From the spectral density function of a response the significant amplitude can be calculated. The significant amplitude is defined to be the mean value of the highest one-third part of the highest wave heights, so:

$$r_{a\,1/3} = 2.\sqrt{m_{or}} \tag{2.16}$$

A mean period can be found from the centroid of the spectrum by:

$$T_{1r} = 2.\pi.\frac{m_{or}}{m_{1r}} \tag{2.17}$$

Another definition, which is equivalent to the average zero-crossing period, is found from the spectral radius of inertia by:

$$T_{2r} = 2.\pi\sqrt{\frac{m_{or}}{m_{2r}}} \tag{2.18}$$

The probability density function of the maximum and minimum values, in case of a spectrum with a frequency range that is not too wide, is given by the Rayleigh distribution:

$$f(r_a)=\frac{r_a}{m_{or}}.\exp\{\frac{-r_a^2}{2.m_{or}}\}.dr_a \tag{2.19}$$

This implies that the probability of exceeding a threshold value a by the response amplitude r_a becomes:

$$P\{r_a > a\} = \int_a^\alpha \frac{r_a}{m_{or}}.\exp\{\frac{-r_a^2}{2.m_{or}}\}.\,dr_a$$

$$= \exp\{\frac{-a^2}{2.m_{or}}\} \tag{2.20}$$

The number of times per hour that this happens follows from:

$$N_{hour} = \frac{3600}{T_{2r}}.P\{r_a >\} \tag{2.21}$$

The spectral value of the waves $S_\zeta(\omega_e)$, base on ω_e, is not equal to the spectral value $S_\zeta(\omega)$, based on ω. Because of the requirement of an equal amount of energy in the frequency bands $\Delta\omega_e$ and $\Delta\omega$, it follows:

$$S_\zeta(\omega_e)\,.d\omega_e = S_\zeta(\omega).\,d\omega \tag{2.22}$$

From this the following relations is found:

$$S_\zeta(\omega_e)=\frac{S_\zeta(\omega)}{d\omega_e / d\omega} \tag{2.23}$$

The relations between the frequency of encounter and the wave frequency, of which is

$$\omega_e = \omega - k.V.\cos\mu \tag{2.24}$$

From the relation between ω follows:

$$\frac{d\omega}{d\omega} = 1.0 - \frac{V.\cos\mu}{d\omega / dk}$$

The derivative $d\omega / dk$ follows from the relation between ω and k:

$$\omega = \sqrt{k.g.\tanh[k.h]} \tag{2.25}$$

So:

$$\frac{d\omega}{dk} = \frac{g.\tanh[k.h] + \dfrac{k.g}{h.\cosh^2[k.h]}}{2.\sqrt{k.g.\tanh[k.h]}} \tag{2.26}$$

$d\omega_e / d\omega$ can approach from both sides, a positive or a negative side, to zero. As a result of this, around a wave speed equal to twice the forward ship speed component in the direction of the wave propagation, the transformed spectral values will range from plus infinite to minus infinite. This implies that numerical problems will arise in the numerical integration routine.

This is the reason why the spectral moments have to be written in the following format:

$$m_{or} = \int_{o}^{\infty} S_r(\omega_e).d\omega_e \qquad = \int_{o}^{\infty} S_r(\omega).d\omega$$

$$m_{1r} = \int_{o}^{\infty} S_r(\omega_e).\omega_e.d\omega_e \qquad = \int_{o}^{\infty} S_r(\omega).\omega_e.\, d\omega$$

$$m_{2r} = \int_{o}^{\infty} S_r(\omega_e).\omega^2.d\omega_e \qquad = \int_{o}^{\infty} S_r(\omega).\, \omega_e^2.d\omega$$

With:

$$S_r(\omega) = \left(\frac{r_a}{\zeta_a}\right)^2 .\, S_\zeta(\omega) \qquad (2.27)$$

If $S_r(\omega)$ has to be known, for instance for a comparison of the calculated response spectra with measured response spectra, these values can be obtained from this $S_r(\omega)$ and the derivative $d\omega_e / d\omega$. So an integration of $S_r(\omega_e)$ over ω_e has to be avoided.

Because of the linarites, the calculated significant values can be presented by:

$$\frac{r_{a\,1/3}}{H_{1/3}} \text{ versus } T_1, or\, T_2 \qquad (2.28)$$

With

$H_{1/3}$ *significant wave height*

$T_{1,} T_2$ *average wave periods*

2.1.3 Resistance (R_T)

As a ship moves through calm water, the ship experiences force acting opposite to its direction of motion. This force is the water's resistance to the motion of the ship, which is referred to as "total hull resistance" (R_T). It is this resistance force that is used to calculate a ship's effective horsepower, [4]. A ship's calm water resistance is a function of many factors, including ship speed, hull form (draft, beam, length, wetted surface area), and water temperature.

2.1.4 Components of Ship Hull Resistance

As a ship moves through calm water, there are many factors that combine to form the total resistance force acting on the hull. The principal factors affecting ship resistance are the friction and viscous effects of water acting on the hull, the energy required to create and maintain the ship's characteristic bow and stern waves, and the resistance that air provides to ship motion. In mathematical terms, total resistance can be written as:

$$R_T = R_V + R_W + R_{AA} \qquad (2.29)$$

Where:

R_T = total hull resistance

R_V = viscous (friction) resistance

R_W = wave making resistance

R_{AA} = air resistance caused by ship moving through calm air other factors affecting total hull resistance can also be presented.

2.1.5 Dimensionless Coefficients

Naval architects use many dimensionless coefficients to describe the design and performance of a ship's hull. Dimensionless coefficients allow the naval architect to compare model test data to full-scale ship data, or to compare the performance of several ship types. The field of ship resistance and propulsion makes extensive use of standard dimensionless coefficients, [6]. The derivation of these standard coefficients is accomplished through dimensional analysis. Just as total hull resistance is the sum of viscous, wave making, and air resistance, we can write an equation for total resistance in terms of dimensionless coefficients.

$$C_T = C_V + C_W \qquad (2.30)$$

Where: C_T = coefficient of total hull resistance

C_V = coefficient of viscous resistance

C_W = coefficient of wave making resistance

$$C_T = \frac{R_T}{1/2\rho V^2 S} \qquad (2.31)$$

Where,

R_T = Total hull Resistance

ρ = Water density $kg/m^{2)}$

V = Velocity (ship speed) (m/s)

S = Wetted surface area of the underwater hull (m^2)

Naval architects also use a dimensionless form of velocity called the Froude number (fn).

$$F_n = \frac{V}{\sqrt{gL}} \qquad (2.32)$$

Where,

V = Velocity (ship speed) (m/s)

g = Acceleration of gravity (m/s^2)

L = Length of the ship (m)

Mathematically, laminar and turbulent flow can be described using the dimensionless coefficient known as the Reynolds Number:

$$R_n = \frac{LV}{\nu} \qquad (2.33)$$

where:

R_n = Reynolds number

L = Length of ship (m)

V = Velocity (ship speed) (m/s)

ν = Kinematic Viscosity of water (m^2/s)

2.1.6 Viscous Resistance (R_V)

The increase in resistance due to pressure is called "viscous pressure drags" or "form drag", and is sometimes also referred to as the normal component of viscous resistance. Ships that are short in length with wide beams (a low length to beam ratio) will have greater form drag than those with a larger length to beam ratio. Also, ships that are fuller near the bow (e.g., bulk oil tanker) will have greater form drag than ships with fine bows (e.g., destroyer). Ships are often designed to carry a certain amount of payload (weight and volume) at a given speed. Therefore, the means of reducing Viscous Resistance for a design is to reduce the coefficient of viscous resistance or to reduce the surface area for a given volume.

$$R_v = C_v \times K \quad (2.34)$$

$$K = \frac{1}{2} \times \rho \times V^2 \times A_s \quad (2.35)$$

Where,
C_v = Coefficient of viscous resistance or dimensionless coefficient
K = Reference force

2.1.6 Frictional Resistance (Rf)

Experimental data have shown that water friction can account for up to 85% of a hull's total resistance at low speed ($F_n \leq 0.12$ or speed-to-length ratio less than 0.4 if ship speed is expressed in knots), and 40-50% of resistance for some ships at higher speeds. The friction resistance can increase considerably for rough surfaces. For new ships, the effect of roughness is included in the ITTC line or the correlation constant. A rough hull surface (without fouling) increases the frictional resistance by up to 5%. Fouling can increase the resistance by much more. However, modern paints prevent fouling to a large extent and are also self-polishing.

$$R_F = C_F \times K \quad (2.36)$$

Where,
C_f = Coefficient of frictional resistance or dimensionless coefficient
K = Reference force

2.1.7 Air Resistance (R_{AA})

Air resistance is the resistance caused by the flow of air over the ship with no wind present. Resistance due to air is typically 4-8% of the total ship resistance, but may be as much as 10% in high sided ships such as aircraft carriers. Attempts have been made reduce air resistance by streamlining hulls and superstructures, however; the power benefits and fuel savings associated with constructing a streamlined ship tend to be overshadowed by construction costs.

$$R_A = C_A \times K \quad (2.37)$$

Where,
C_A = Coefficient of Air Resistance
K = Reference force
or

$$R_A = 0.90 \times \frac{1}{2} \times \rho_{air} \times V^2 \times Air \quad (2.38)$$

Where,
ρ_{air} = Density of air
Air = cross – sectional area of vessel above the water
V^2 = Vessel speed

2.1.8 Wave Making Resistance (R_W)

The second major component of hull resistance is the resistance due to wave making. The creation of waves requires energy. Froude's 1877 sketch of the wave patterns produced by a ship is compared to the photographs of actual to note the similarities. Such predictions for a certain region or route depend on the accuracy of sea state statistics which usually introduce a larger error than the actual computational simulation.

$$R_W = C_W \times K \quad (2.39)$$

Where,
C_W = Coefficient of wave making resistance
K = Reference force

2.1.9 Effective Power

The effective power at any speed is defined as the power needed to overcome the resistance of the naked hull at that speed, it is sometimes referred to as the low rope power that would be expanded if the ship were to be towed through the water without the flow around it being affected by the means of towing another, higher effective power would apply if the ship to wave has a poor hydrodynamic performance, [9]. For a given speed the effective power is the product of the total resistance and the vessel speed thus,

$$P_E = R_T\,(KN) \times V_s\,(m/s) \quad (2.40)$$

The fuel consumption, FC, of a hull is proportional to the product of R_T and the speed experienced by the vessel hull.

$$FC = P_E \times sfc$$
$$= R_T\,(KN) \times V(m/s) \times Sfc\left(\frac{grams}{kw.s}\right) \quad (2.41)$$

2.2 MATERIALS

2.2.1 Bourbon-Helene

Bourbon Helene is an **Offshore Tug/Supply Ship** registered and sailing under the flag of **Panama.** Her gross tonnage is **2535** and deadweight is **2879** built in **2006** with length overall (LOA) of **73.2** m and beam of **16.5** m.

The vessel is designed for world-wide, deep-water operations to fulfil the following duties:

a) Light subsea works and deep-water precision lifting up to 1,900 m
b) ROV operations and survey operations.

2.2.2 Ship Dimensions Particulars

Length of ship	**73.2** m
Breadth moulded	**16.5** m
Depth	6.80 m
Draft (Max)	5.5 m
Deadweight at max. draft	2879 t

2.2.3 Hydrodynamics Analysis

A design of a modern big ship starts from hydrodynamics analysis, fuel saving, power estimation, passenger comfortability and structural safety operational handling are all solved using hydrodynamics knowledge, [7]. Finding the forces on the ship when it is restrained from motion and subjected to irregular or regular waves. The forces acting on the body are:

- ❖ The Froude–Krylov force, which is the pressure in the undisturbed waves integrated over the wetted surface of the ship.
- ❖ The Diffraction forces, which are pressures that occur due to the disturbances in the water because of the ship being present.

Finding the forces on the ship when it is forced to oscillate in still water conditions. The forces are divided into:

- ❖ Added mass forces due to having to accelerate the water along with the ship.
- ❖ Damping forces due to the oscillations creating outgoing waves which carry energy away from the ship.
- ❖ Restoring forces due to bringing the buoyancy/weight equilibrium out of balance.

2.2.4 Autodesk Analysis

Autodesk Inventor is a computer-aided design application for 3D mechanical design, simulation, visualization, and documentation to view them in 2D and 3D which was used to design the parent and optimised hull in appendix (vi) in solid form. This software incorporates integrated motion simulation and assembly stress analysis, whereby users are given options to input driving loads, dynamic components, friction loads and further run the dynamic simulation to test how the product will function in a real-world scenario.

2.2.5 SACs Marine Analysis

The SACS Marine Enterprise Add-on provides modelling of vessel hulls, calculation of stability, and prediction of vessel motions. The package contains the Hull Modeler, Hull Mesher, Motions, and Stability modules, and requires the use of the Offshore Structure, Offshore Structure Advanced, or Offshore Structure Enterprise package. SACS Motions is an integrated sea keeping analysis and motion prediction module using either standard Strip Theory or panel-based radiation-diffraction methods to predict vessel motions. Hull Modeler contains a full range of tools optimized for hull shape creation and modification, [13]. The full suite has all the functionality of SACS Marine plus integrated hull modelling, intact and damage stability analysis, and six degrees of freedom motions prediction.

2.2.6 Hull Modelling Analysis

SACs Modeler provides fast, flexible, and intuitive modelling of all types of hulls, superstructures, and appendages. An unlimited number of trimmed NURB surfaces can be used to model any vessel from yachts to workboats to the largest ships, [14]. The Modeler design module enables naval architects to create optimized hull forms quickly and accurately. Any number of NURB surfaces can be joined, trimmed, and manipulated to create a complete model ready for hydrostatic and performance analysis or construction detailing. SACS Hull Modeler allows you to model any type of vessel hull shape, [8]. Using trimmed 3D NURB surface technology, Hull Modeler contains a full range of tools to optimized hull shape creation and modification.

2.2.7 Hydrostatic and Stability Analysis

The SACs Stability module provides fast, graphical, and interactive calculation of intact and damaged stability and strength for all types of SACs designs and for estimating for the hydrostatic parameters in appendixes A and B. Once a desired hull form is created using Modeler, its stability and strength characteristics can be assessed using the Stability analysis module, [10]. The Stability analysis module provides a range of powerful analysis capabilities to handle all types of stability and strength calculations and also hydrostatic parameters for any ship.

All functions within the Stability interface of Appendixes (xi) are performed using a graphical multi-window environment consistency with all other SACs modules. Data is displayed simultaneously in graphical and tabular form and is automatically updated when changes are made and as the analysis progresses. An integrated load case editor makes setting up any number of loading conditions simple and error free. Copying and pasting data to and from spread sheets also makes it easy to prepare complex loading schedules in other programs and run them in Stability.

Volume of displacement : ∇ (2.42)

Waterline area : A_{WL} (2.43)

Block coefficient, L_{WL} based : $C_{B,WL} = \dfrac{\nabla}{l_{WL}\ x\ B_{WL}\ x\ D}$ (2.44)

Mid ship section coefficient : $C_{WL} = \dfrac{A_W}{B_{WL}\ x\ D}$ (2.45)

Longitudinal prismatic coefficient : $C_p = \frac{\nabla}{A_w \ x \ L_{WL}}$ (2.46)

Water plane area coefficient : $C_{WL} = \frac{A_{WL}}{L_{WL} \ x \ B_{WL}}$ (2.47)

Length between perpendiculars : $L_{PP} = 0.97 \ x \ L_{WL}$ (2.48)

2.2.8 Vessel Motion Analysis

The SACs Motions module for hydrodynamic and sea keeping analysis provides fast, reliable calculation of the various RAO of the vessel responses in chapter (4) and sea keeping characteristics for the variety of the parent hull and the optimised hull form designs created with SACs Modeler.

2.2.9 Resistance Analysis

The SACs Resistance module interface which is an integral part of the motion modular estimates the resistance requirements for any SACs design using industry standard prediction techniques. SACs Resistance can also compute the resistance and wave making of slender vessels using an integrated potential flow solver, [12]. When designing a vessel using SACs, the Resistance module's calculation methods help you estimate the resistance and powering requirements of the hull. SACs Resistance module includes industry-standard algorithms, allowing you to select the methods most appropriate for your hull shape.

3 RESULTS AND DISCUSSIONS

3.1 Sacs Motion Analysis

3.1.1 Initial and Optimized Hull Form Data at Different Sea State

Sacs motion Analysis program based on Strip Theory and MATLAB code was used in achieving the RAOs graphs and Table (3.1), (3.2), (3.3) and (3.4) readings from the initial and optimised hull form and to analyse the various events on the behaviour of the vessel at sea. The study includes the linear sea keeping analysis, coupled with the ship movement in the six degrees of motion at varying forward speed between 180 and 135° incidence angle with JONSWAP wave power density spectrums which always have a peak enhancement factor of 1.0deg/sec to 5.0deg/sec respectively.

TABLE (3.1) Initial Hull Form Data (1) at 180-Degree Sea

S/N	Speed (m/s)	Speed (Knots)	Deg (0)	Period (s)	Wave Height (m)	Resistance (KN)	Displacement (m³)	Power (KW)
1.	0	0	180	9.997	4	1584.667	9918.253	0
2.	2.57	5	180	9.997	4	1347.719	9918.253	3463.64
3.	5.14	10	180	9.997	4	1154.906	9918.253	5936.22
4.	7.71	15	180	9.997	4	990.076	9918.253	7633.49
5.	10.28	20	180	9.997	4	847.247	9918.253	8709.60
6.	11.82	23	180	9.997	4	771.156	9918.253	9116.61
7.	12.85	25	180	9.997	4	724.326	9918.253	9307.59

Table (3.2) Initial Hull Form Data (2) at 135-Degree Sea

S/N	Speed (m/s)	Speed (Knots)	Deg (0)	Period (s)	Wave Height (m)	Resistance (KN)	Displacement (m³)	Power (KW)
1.	0	0	135	9.997	4	1481.919	9918.253	0
2.	2.27	5	135	9.997	4	1331.856	9918.253	3422.87
3.	5.14	10	135	9.997	4	1207.515	9918.253	6206.63
4.	7.71	15	135	9.997	4	1096.043	9918.253	8450.49
5.	10.28	20	135	9.997	4	992.829	9918.253	10206.28
6.	11.82	23	135	9.997	4	934.245	9918.253	11044.64
7.	12.85	25	135	9.997	4	896.502	9918.253	11520.05

TABLE (3.3) Optimized Hull Form Data (3) at 135-Degree Sea

S/N	Speed (m/s)	Speed (Knots)	Deg (0)	Period (s)	Wave Height (m)	Resistance (KN)	Displacement (m³)	Power (KW)
1.	0	0	135	9.997	4	471.859	3407.940	0
2.	2.57	5	135	9.997	4	429.499	3407.940	1103.81
3.	5.14	10	135	9.997	4	395.224	3407.940	2031.45

4.	7.71	15	135	9.997	4	365.157	3407.940	2815.36
5.	10.28	20	135	9.997	4	338.281	3407.940	3477.53
6.	11.82	23	135	9.997	4	323.866	3407.940	3828.09
7.	12.85	25	135	9.997	4	315.033	3407.940	4048.17

TABLE (3.4) Optimized Hull Form Data (4) at 180-Degree Sea

S/N	Speed (m/s)	Speed (Knots)	Deg (0)	Period (s)	Wave Height (m)	Resistance (KN)	Displacement (m³)	Power (KW)
1.	0	0	180	9.997	4	478.323	3407.940	0
2.	2.57	5	180	9.997	4	422.088	3407.940	1084.7
3.	5.14	10	180	9.997	4	378.615	3407.940	1946.0
4.	7.71	15	180	9.997	4	341.094	3407.940	2629.8
5.	10.28	20	180	9.997	4	308.707	3407.940	3173.5
6.	11.82	23	180	9.997	4	291.322	3407.940	3443.4
7.	12.85	25	180	9.997	4	280.354	3407.940	3602.5

The Tables (3.1), (3.2), (3.3) and (3.4) was used to plots the vessel speed to resistance and speed to power graphs which illustrate the hull's motion based on the direction of the waves interacting with the hull oriented between 180 degrees and 135 degrees, the speed of the ship which increases from 0 knots to 25 knots shows that the heave and pitch response is higher in forward speed while the roll motion is highest in the still sea. From the results, it is noted that roll has a peaky response spectrum in the region near to its natural frequency. The RAOs for heave and pitch are quite consistent with their maximum responses occurring near their natural frequencies. The results indicate that the choice of hydrodynamic performance depends on the hull form and nature of seakeeping analysis for it which can offer a simple, practical, and realistic assessment in comparative sea keeping studies. Finally, the main analysis of the initial and optimized results in which the optimized analysis gave a more satisfactory results obtained is in the form of spectral analysis of wave and hull motions used to obtain the different RAOs which is the key to all sea keeping analysis.

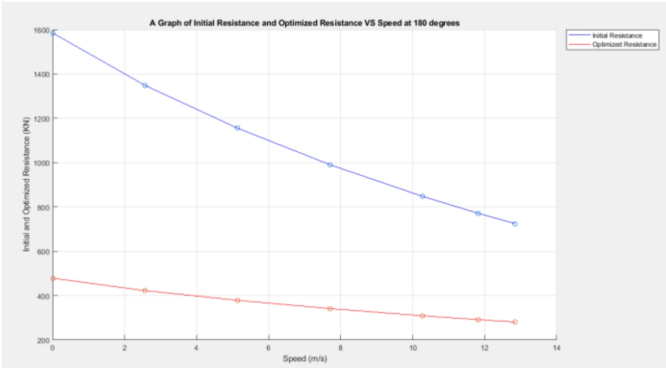

Figure (3.1): Graph of Variation of Ship Speed vs Power for the Initial and Optimized Hull at 180-Degree Sea

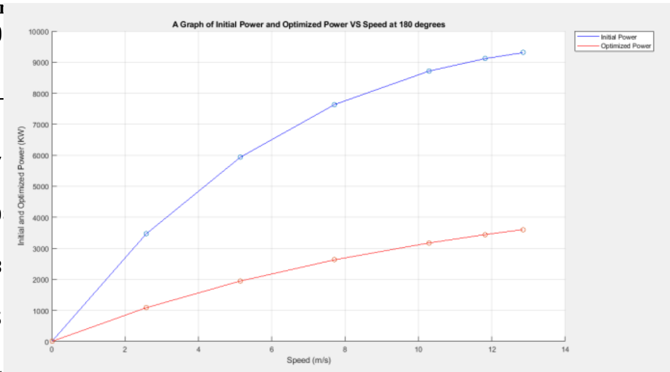

Figure (3.2): Graph of Variation of Ship Speed Vs Resistance for the Initial and Optimized Hull at 180-degree sea

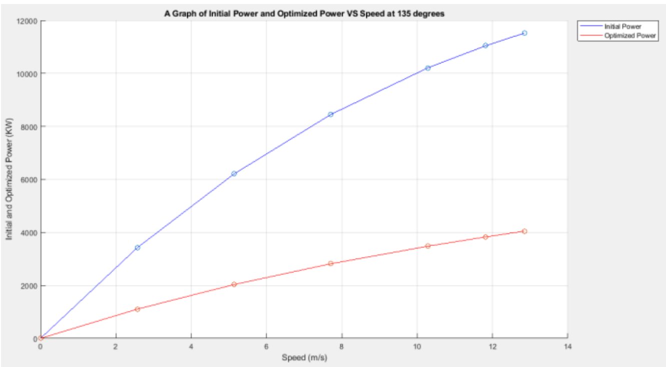

Figure (3.3): Graph of Variation of Ship Speed vs Power for the initial and optimized hull at 135-degree sea

As a ship moves at various speed through the water as illustrated on Fig (3.1), (3.2), (3.3), and (3.4) the ship experiences a force acting opposite to its direction of motion. This force is the water's resistance to the motion of the ship, which is referred to as "total hull resistance" (R_T). A ship's water resistance is a function of many factors, including ship speed, hull form (draft, beam, length, wetted surface area), and water temperature from the above graph resistance increases as speed reduces higher that makes resistance curve not linear, but reduces more steeply at higher speeds leading this to increase in power which is felt directly in the amount of fuel burned during the transit. A ship's fuel consumption curve is similar in shape to its horsepower and total resistance curves consistence voyage requires careful attention during transit and fuel consumption rates to ensure that the ship arrives at its destination with an adequate supply of fuel onboard at a required service speed of the vessel.

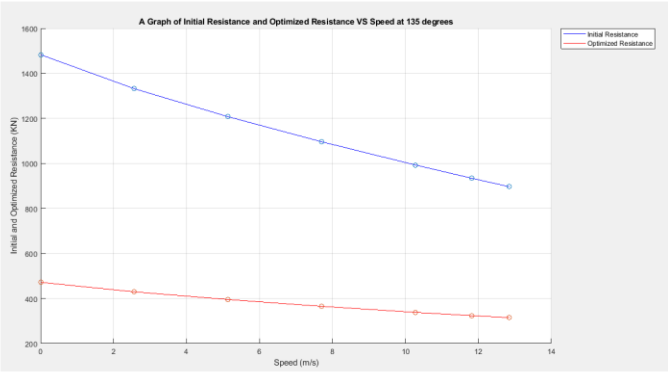

Figure (3.4): Graph of Variation of Ship Power vs Resistance for the initial and optimized hull at 135-Degree Sea

The resistance of the optimized hull and initial hull form were calculated under the same conditions by using MATLAB, the total resistances for optimized hull are acceptable due to the positive effect from the bulbous designed into it which has given it a better performance and reduction in resistance. Ships use large quantities of fuel to provide the necessary propulsive power to overcome resistance in their motion across ocean surfaces. The optimized grid results are in very close agreement with the predicted resistance and power which was significantly reduced when compared with the initial hull estimated result, so the bulbous design with SACs NURBs generation method is acceptable since the predictions of the overall analytical scheme is suitable for the resistance prediction. Bulbous designed into the bow side of the hull was to achieve a decrease in the wave making resistance of the ship. It can be observed from the comparisons that the optimized hull with a reduce resistance, not only because it has simple geometrical form but with a good mathematically defined shape. This may serve as a basis for application of such approach to optimization of ship hull form and improvement of its propulsion efficiency.

The objective of this study is to analyse on resistance against power to achieve a good hydrodynamic performance of the ship hull. The range of vessel headings analysis which was varied from 180 to 135° using increment vessel headings of 45°produced satisfactory results and the solving time was not excessive.

3.2 Respond Amplitude Operator (RAOs)

The motion Analysis program based on Strip Theory and MATLAB code was used in achieving the RAOs graphs and Table (3.1), (3.2), (3.3) and (3.4) readings for the initial and optimised hull form and to analyse the various events on the behaviour of the vessel at sea. The study includes the linear sea keeping analysis, coupled with the ship movement in the six degrees of motion at varying forward speed between 180 and 135° incidence angle with JONSWAP wave power density spectrums which always have a peak enhancement factor of 1.0deg/sec to 5.0deg/sec respectively.

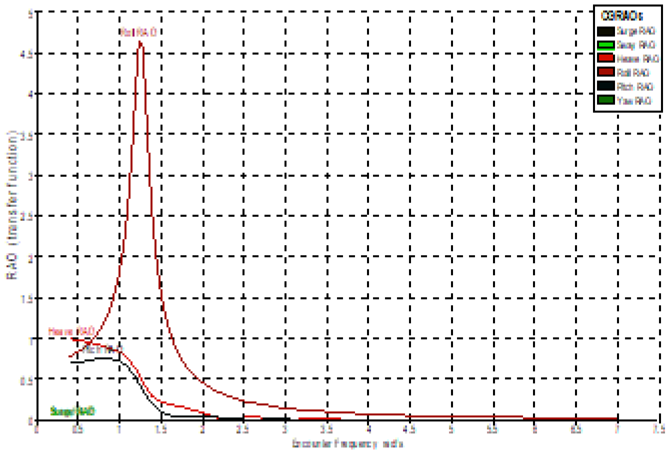

Figures (3.5) Graph of pitch, heave and roll RAOs response at 180-degree sea and at 15 knots (7.71 m/s) forward speed for the optimized and initial hull form

Figures 3.5 the maximum value of RAOs is observed in the pitch and heave motion. From the stability result of the supply ship, any value of well over 1.0deg/sec of the RAO can cause significant change in the vessel stability. For a RAO less than 1.0deg/sec of the angle of inclination to 1 rad/s of wave amplitude is not too much. It means that the ship can remain stable. However, favoring the operational condition of the Sea.

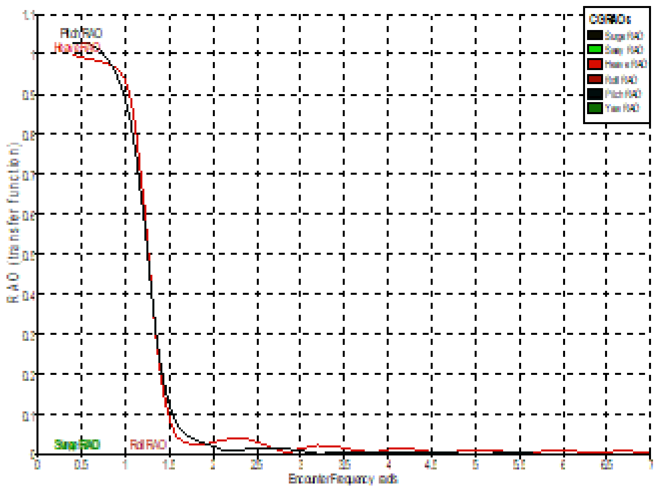

Figures (3.6): Graph of roll, heave and pitch RAOs response at 135-degree sea and at 15 knots (7.71 m/s) forward speed for the optimized and initial hull form

Figure 3.6 presents the RAO of the supply ship in roll, pitch and heave motion for different response sat encounter of the wave. The pitch is reasonably well behaved and increases from zero at short periods, the heave and roll have natural period within the range of periods plotted and could have resonance only in high wave periods. This means that the acceleration will not cause high seasickness for the ship crew. However, the data from the analysis suggests a tendency for the peak value to move to slightly higher dimensionless encounter-frequency as the ship moves further against sea direction.

4. CONCLUSIONS

This paper demonstrates the investigation on the hydrodynamic performance of the initial and optimised hull form of a parent ship from the resistance, power and sea keeping point of view. Based on the analytical results, it was noted that the resistance results of the optimised hull are lower than the initial hull at different speeds under the same conditions.

Also, it may be seen that the RAOs for the optimised hull are less than the initial hull form. Minimum fuel consumption and maximum comfort on board (minimum vibration and noise) are usually the primary targets in ship hull design. It has been demonstrated that minimizing the total resistance by obtaining a very hull form design to sustain a given speed is a better goal than minimizing the power.

REFERENCES

[1] Abt, C. & Harries S. A (2017). New Approach to Integration of CAD and CFD for Naval Architects.

[2] B´ezier P. (1974). Mathematical and Practical Possibilities of UNISURF. In Computer Aided Geometric Design.

[3] Bole, M. & Forrest C. (2005). Early Stage Integrated Parametric Ship Design. In Proceedings of the 12th International Conference on Computer Applications in Shipbuilding (ICCAS 2005), Busan, South Korea.

[4] Casteljau, F. de (1959). Outillage Methodes Calcul. Technical report, Andre Citroen Automobiles SA, Paris.

[5] Chakraborty Soumya (2000). In proceedings of the 6th International Conference on Computer Applications and Information Technology in the Maritime Industries (COMPIT2007).

[6] Evans J. H. (1959). Basic Design Concepts. Naval Engineers Journal, (pp71) 671–678.

[7] Gordon, W. and Risenfield R. (1974.). B-spline Curves and Surfaces. In Barnhill and Riesefield, editors, Computer Aided Geometric Design. Academic Press.

[8] Harries, S. C & Hochkirch K. (2004). Modelling Meets Simulation Process Integration to Improve Design. In Honorary Colloquium for Professor Hagen, Schluter and Thiel.

[9] Harries. S. (1998). Parametric Design and Hydrodynamic Optimization of Ship Hull Forms. Institute of Naval Architecture and Ocean Engineering, Technische University Berlin.

[10] Mistree, F. Smith, W. F and Muster D. (1990). Decision-Based Design: A Contemporary Paradigm in Ship Design. Transactions of the Society of Naval Architects and Marine Engineers (SNAME).

[11] Peacock, D. A. (2018). Decision-Based Hydrodynamic Design of Displacement Monohulls. PhD thesis, School of Mechanical and Manufacturing Engineering.

[12] Reed, A. & Nowicki, H. (1972). Interactive Creation of Fair Ship Lines. Journal of Ship Research, Access Science McGraw-Hill ship design spiral webpage.

[13] Rogers, D. F, Satterfield, S. & Rodriguez. F. (1983). Ship Hulls, B-spline Surfaces, and CAD/CAM. IEEE Computer Graphics and Applications.

[14] Shapiro, V. (2002) Solid Modelling. Elsevier Science Publishers.